Dianionic amidinates at silicon and germanium centers: Four-, six- and eight-membered rings

Thomas Segmüller [a], Peter A. Schlüter [a], Markus Drees [b], Annette Schier [a], Stefan Nogai [a], Norbert W. Mitzel [c], Thomas Straßner [b,*], Hans H. Karsch [a,*]

[a] *Department Chemie, TU München, Lichtenbergstr. 4, 85747 Garching, Germany*
[b] *Professur für Physikalische Organische Chemie, TU Dresden, Mommsenstr. 13, 01062 Dresden, Germany*
[c] *Institut für Anorganische und Analytische Chemie, Universität Münster, Corrensstr. 30, 48149 Münster, Germany*

Abstract

At variance to an earlier finding, the reaction of Me_2SiCl_2 with $Li[(Me)N–C(Ph)–NH]$ (**1a**), in the presence of a base, gives a six-membered ring molecule μ-[(Ph)(MeN)C–N][–SiMe$_2$–N–C(Ph)–N(Ph)–SiMe$_2$–] (**s3a**), whereas with $Li[^{i}PrN–C(Ph)–NH]$ (**1b**), a four-membered ring molecule μ-[^{i}PrN(Ph)C–N]$_2$(SiMe$_2$)$_2$ (**s4b**) was formed. In contrast, with $Li[^{t}BuN–C(Ph)–NH]$ (**1c**), no such reaction occurred. Obviously, a delicate influence of steric effects has to be taken into account. In fact, the latter amidinate reacts with $GeCl_2$ to form an eight-membered ring molecule [^{t}BuN–C(Ph)–N–Ge]$_4$ (**5c**) without adding an additional base.

The compounds are fully characterized and their structures determined by X-ray diffraction. DFT calculations confirm the dependence on steric influences. The relative energies of ground and transition states give a rationalization the ease of transformations of the various rings *via* pathways with penta- and hexacoordinate silicon centers, which in turn relates to the experimental results on penta- and hexacoordinate silicon amidinates and their fluctional behavior in solution.
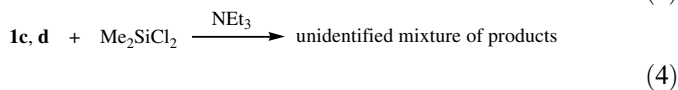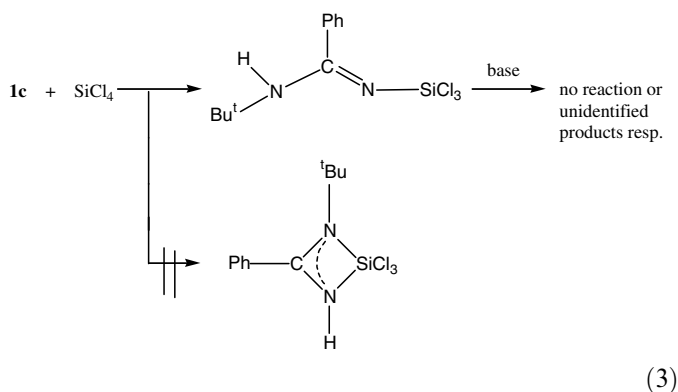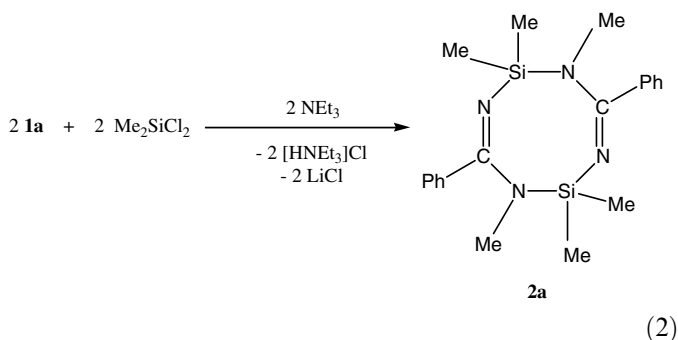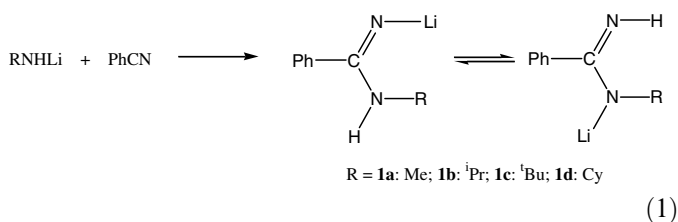© 2007 Elsevier B.V. All rights reserved.

1. Introduction

Dianionic amidinates at (organo-)silicon centers are potentially useful to form polymers with $[(R)N–C(Ph)–N]^{2-}$ linkages, mimicking O^{2-} bridges in silicones or silicates in one-, two- or three-dimensional frameworks. This dianionic amidinate should be obtained by the reaction of the monoanionic, unsymmetrical amidinates $[(R)N–C(R')–NH]^{-}$, in turn easily prepared ($R' = Ph$) by reacting LiNHR with PhCN (Eq. (1)), followed by a reaction with (organo)silicon chlorides and subsequent deprotonation by means of a suitable base. Other (organo)element chlorides (*e.g.* BCl_3, $AlCl_3$, $TiCl_4$, *etc.*) could modify the poly-

mers and, again in principle, give rise to ceramic materials with designed properties by thermolysis. In principle, this concept, though then not intended for the indicated purpose, was realized in an early study of the reaction of Me_2SiCl_2 with $Li[MeN–C(Ph)–NH]$, obtained *in situ* from LiNHMe and PhCN, in the presence of a base [1]. This reaction, performed at room temperature, was accompanied by "fume evolution" and was believed to yield an eight-membered ring molecule, **2a**, in 43% (Eq. (2)), by a questionable analysis of the ^{1}H NMR spectrum (60 MHz, CW, r.t.). Nevertheless, besides of the exact constitution of this compound, the report seemed reliable enough to assume the presence of a dianionic amidinate as bridging ligand between two silicon centers and thus gave a hint that the above-mentioned concept seemed feasible.

---

* Corresponding authors.
   E-mail address: Hans.H.Karsch@lrz.tum.de (H.H. Karsch).

RNHLi + PhCN ⟶ [structure] R = **1a**: Me; **1b**: ⁱPr; **1c**: ᵗBu; **1d**: Cy

$$(1)$$

2 **1a** + 2 Me₂SiCl₂ →[2 NEt₃][− 2 [HNEt₃]Cl − 2 LiCl] [structure **2a**]

$$(2)$$

1c + SiCl₄ ⟶ [structure] →[base] no reaction or unidentified products resp.

$$(3)$$

**1c, d** + Me₂SiCl₂ →[NEt₃] unidentified mixture of products

$$(4)$$

Earlier work by us [2,3] has shown, however, that there is obviously a severe steric problem: the reactions of amidinates **1c** and **1d** with silicon centers under deprotonation conditions could not be achieved with various bases and/ or clear results were not obtained (Eq. (4)). Therefore we decided to reinvestigate reaction (2) and include also the reaction with **1b**. Preliminary results have been reported [4,5].

To get insight into the steric influence of the substituents on the preferred ring size we calculated the energies of isomers with different ring size and the transition states for the ring size changes. We intent to get an explanation why the change of the substituent (alkyl or aryl) leads to different crystal structures.

2. Results and discussion

The lithium amidinate **1a** [1,3,6], prepared from Me₂NLi and PhCN was allowed to react *in situ* with Me₂SiCl₂ in the presence of NEt₃ in Et₂O solution according to Scherer's procedure (Eq. (2)). Whereas repeated reactions conducted at room temperature did not lead to reproducible reactions,

an experiment at −78 °C led to the formation of colorless crystals of compound **s3a** isolated in 89.6% yield (Eq. (5)).

2 **1a, 1b** →[+ 2 Me₂SiCl₂][+ 2 NEt₃]

R = Me [structure **s3a**]

R = ⁱPr [structure **a4b**]

$$(5)$$
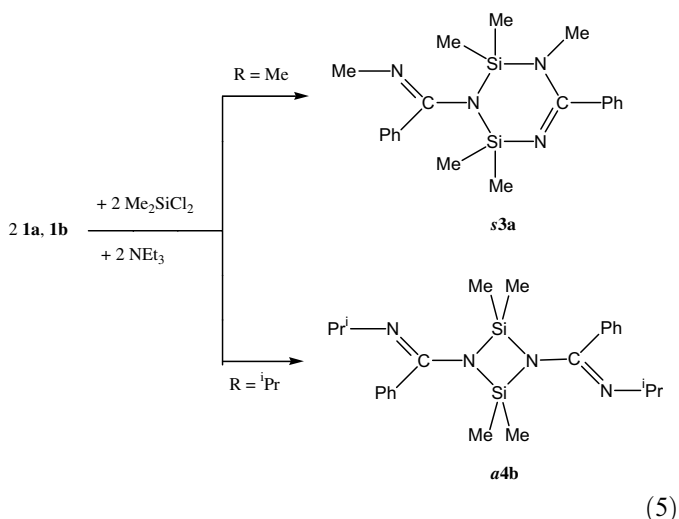
The compound was found to have a dimeric structure [Me₂Si–N–C(Ph)–NMe]₂ (MS), in line with Scherer's formula **2a**, and appears to be stable in solution at room temperature according to the NMR spectra, but with a somewhat different constitution. Unfortunately, we could not draw relevant information from the ¹³C and ²⁹Si spectra, because room temperature spectra showed only broad signals, presumably due to their fluctional behavior. However, in the VT-¹H NMR spectra (200 MHz, FT), fluctional and constitutional effects could be separated. In the temperature range from −80 to 85 °C two SiCH₃ signals with decreasing shift difference were observed, but with equal intensity throughout, which is in line with Scherer's report. Also observed were two independent NCH₃ signals at −60 °C. This hardly is in line with formula **2a**, but rather is consistent with formula **s3a**. Furthermore, the postulation of the presence of two different conformers seems obsolete (a constitutional eight-membered ring isomer could not be ruled out rigorously at this stage, however). Moreover, at −80 °C, one of the two NCH₃ signals is split in turn into two signals (ratio 2:1), which can be interpreted as hint for the steric congestion within the six-membered ring of **s3a** and hence hindered rotation of the N–CH₃ group. From the spectra no information was gained about the rotational behavior (or position) of the external MeNC(Ph)-group, *i.e.* about the presence of **s3a** or **a3a** (*syn* or *anti* rotamers; Eq. (6)).

[structure **s3a**] ⇌[Rotation] [structure **a3a**]

$$(6)$$
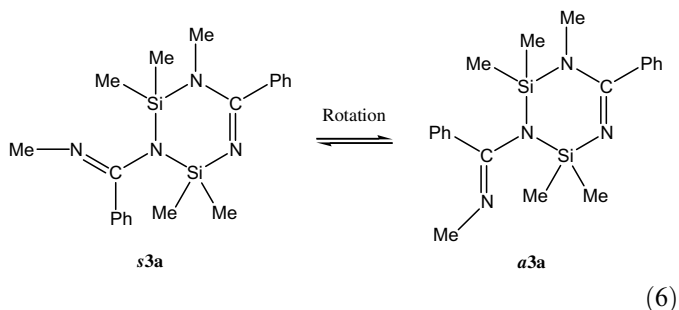
To get more insight into the nature of the compound, or of its possible isomer, a X-ray diffraction study of *s3a* was undertaken.

Colorless crystals of *s3a* (orthorhombic, space group $Pna2_1$, with four molecules/cell) were grown from pentane. The molecular structure, together with selected bond distances and angles, is shown in Fig. 1. The compound consists of two dianionic amidinate ligands and two $SiCl_2$ fragments, one ligand bridges the two silicon atoms by its two nitrogen (N1, N2), the other one by only one nitrogen (N3) atom, whereas the fourth, dicoordinated nitrogen (N4) atom remains uncoordinated. Thus, the tetracoordinated silicon atoms, the almost planar, tricoordinated atoms N1, C1, N3 and the dicoordinated N2 atom form a slightly twisted six-membered ring. Remarkably, the C1–N2 and C2–N4 distances are almost equal and shorter (double bonds) than the other C–N distances (single bonds). The Si–N distances (1.732–1.778 Å, with Si–N2 being the shortest distance) are longer than the short Si–N bonds in other tetracoordinated silicon compounds with non-chelating amidinate ligands (1.625–1.651 Å; see below), but compare well with that in an example with a semi-chelating amidinate ligand (1.735 Å; see below). Two additional features deserve further comment: Firstly, both phenyl rings are

not in plane with the C1 and C2 centered triangles (interplane angles N1–C1–N2/phenyl ring 41.1° and N3–C2–N4/phenyl ring 58.2°), respectively. One explanation would be the repulsive interaction of the rings with the N–CH_3 groups (which is less, however with the N–^iPr groups in *a4b* – see below), thus indicating some steric constraints. Secondly, the rotational position of the "free" amidinate nitrogen atom N4 enables this nitrogen atom to come into contact with the electronically least saturated Si1 atom: Si–N4: 2.713 Å; *cf.*: semi-chelating (unisobidentate): $(CF_3)_2CH$—N≡C$(Cl$—$C_6H_4)N(2,6$-$Me_2C_6H_3)$ —$SiCl_3$: 2.684(4) Å [7]; non-chelating (monodentate): $NH(^tBu)C(Ph)N$–$SiCl_3$ and $[NH(^tBu)C(Ph)N]_2SiCl_2$: Si–N > 3.9 Å [2,8]. This is clearly less than the sum of Si–N van-der-Waals radii (3.7 Å) and characterizes the semi-chelating nature of the respective amidinate ligand and suggests the presence of a simple, low lying pathway to pentacoordination at Si(1), a prerequisite for ring expansion (see below). Also, the angles N4–C2–N3 (116.6(2)°) and C2–N3–Si1 (112.9(1)°) are less than 120°, the four atoms being approximately coplanar. Though not too strongly convincing, all other data describing the coordination sphere around Si1 compared to those of Si2 augment this interpretation ("real" pentacoordination would afford Si–$N_{ax} = 1.92$–1.96 Å [2–5]). In fact, most amidinates tend to form pentacoordinated and even hexacoordinated silicon species and fluctional behavior of pentacoordinate silicon amidinates is a common feature [2–5].

Obviously, since there are steric constraints to be taken into account as earlier mentioned, amidinates **1c** and **1d** are not readily deprotonated at silicon centers with a base. To further clarify the scope of the reaction, **1b** was used (Eq. (5)). The reaction was performed in ether at r.t. Colorless crystals of an again dimeric compound were obtained from toluene solutions of *a4b* (36.5%).

In contrast to *s3a*, the NMR spectra of *a4b* show – independently from temperature – only one (set of) signal(s) for the Si–CH_3 and N[$CH(CH_3)_2$] groups (^1H, {^1H}^{13}C), the ^{29}Si resonance lies at 3.88 ppm. Together with the MS spectrum, the presence of a four-membered ring cyclo-disilazane (diaza-disila-cyclobutane) structure was deduced and finally confirmed by the result of a X-ray diffraction study.

In fact, *a4b* crystallizes in a monoclinic cell ($P2_1/c$) as a centrosymmetric, essentially planar cyclo-disilazane molecule, *i.e.* the amidinate ligands are bound only by one nitrogen atom each to silicon. The molecular structure is shown in Fig. 2, together with selected bond distances. From the structure it is obvious that the two imide units are in anti conformation, indicating that not the *syn* compound *s4b*, but the *anti* *a4b* has been formed. There are no remarkable deviations from the respective data of known compounds of this type [9–18], whereby a common feature are the small N–Si–N and the larger Si–N–Si angles, although in *a4b*, these values lie at the low (83.9(1)°) and the high end (96.2(1)°) with a non-bonding Si...Si distance of

Fig. 1. Molecular structure of compound *s3a* (a: view from above, b: side view; ORTEP drawing with 50% probability ellipsoids). Selected bond distances (Å) and angles (°): Si1–N1 1.780(2), Si1–N3 1.762(2), Si2–N2 1.732(2), Si2–N3 1.755(2), C1–N1 1.388(3), C2–N3 1.403(3), C2–N4 1.287(3); N3–Si1–N1 102.76(9), Si1–N1–C1 118.9(1), N1–C1–N2 123.1(2), C1–N2–Si2 123.4(2), N2–Si2–N3 106.5(1), Si1–N3–C2 112.8(2), Si2–N3–C2 127.6(2), C2–N4–C3 120.4(2).

Fig. 2. Molecular structure of compound *a***4b** (ORTEP drawing with 50% probability ellipsoids. Selected bond distances (Å) and angles (°): Si1–N1 1.760(1), Si1–N1A 1.759(1), N1–C3 1.384(2), N2–C3 1.283(2), Si1...Si1A 2.6180(7); Si1–N1–Si1A 127.50(9), N1–Si1–N1A 83.85(5), Si1–N1–C3 135.82(10), Si1A–N1–C3 127.50(9), C3–N2–C4 119.82(12).

The NMR spectra (^{1}H, {1H}–^{13}C) gave no clear result, because only one (set of) signal(s) was obtained for the respective functional groups of the ligand. Nevertheless, the self-deprotonation was evident from the absence of an N–H signal and the isolation and NMR spectroscopic identification of the amidine NH(^{t}Bu)—C(Ph)=NH. The mass spectrum of **5c** revealed the presence of a tetrameric compound {Ge[(NH)$_2$(^{t}Bu)C(Ph)]}$_4$, but no decision could be made about the true nature: either a cubane like structure [22] or a twisted eight-membered ring within a 16-membered macrocycle (there is a unique structural analogue in tin chemistry [23]) seemed most likely.

2.618(1) Å. As before in **s3a**, the phenyl rings are not in plane with the carbon substituents at C3/C3A. In this case, they are almost perpendicular (interplane angle N1–C3–N2/phenyl ring 84.4°), obviously for steric reasons, excluding electronic interaction. And as well, the exocyclic amidinate nitrogen atoms N2/N2A, forming a double bond to C3/C3A (1.283(2) Å), are not completely "innocent": the four atoms Si1, N1A, C3A, N2A and Si1A, N1, C3, N2 almost form a plane, thus enabling the nitrogen to approach the silicon atom (3.095 Å). This is more than the respective value in **s3a**, but again clearly much less than the covalent radii would suggest. In variance to **s3a**, the four-membered ring of *a***4b** is much less flexible and thus cannot adapt to the needs for a pre-pentacoordinated conformation at silicon. This in turn explains the increase in ring size for *a***4b** to be a somewhat more energetic pathway than in **s3a** (see DFT calculations).

It emerges from these findings that (small) steric changes exert a dominant influence on the nature of products; bigger groups prevent double deprotonation of amidines at all. To reduce this steric hindrance, we tested the same type of reaction at a somewhat bigger, but comparable coordination center: we replaced Si(IV) by Ge(II). Germanium (II) has been demonstrated to be a suitable coordination center for amidinates [2,4,19–21]. And indeed, by reacting GeCl$_2$ · dioxane with the then sterically unfavorable amidinate **1c**, no addition of another base was required for deprotonation, due to spontaneous deprotonation by a second equivalent of **1c** and **5c** was obtained as colorless crystals from toluene (Eq. (7)) [3,5]

$$\text{Li[NH(}^t\text{Bu)-C(Ph)=N]} + \text{GeCl}_2 \cdot \text{C}_4\text{H}_8\text{O}_2 \xrightarrow[-78°C]{\text{Et}_2\text{O}} 1/4 \ \{\text{Ge[N(}^t\text{Bu)C(Ph)N]}\}_4 \quad (7)$$

$$\textbf{1c} \qquad\qquad\qquad\qquad\qquad\qquad\qquad \textbf{5c}$$

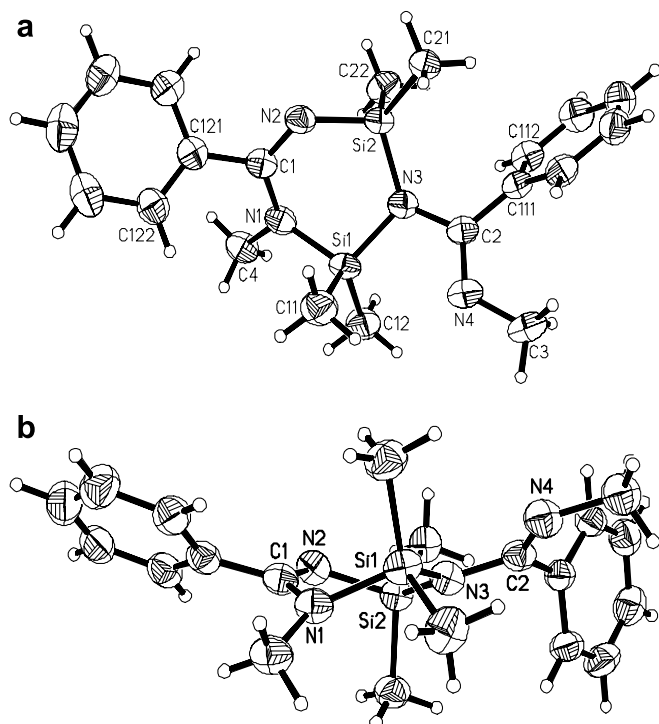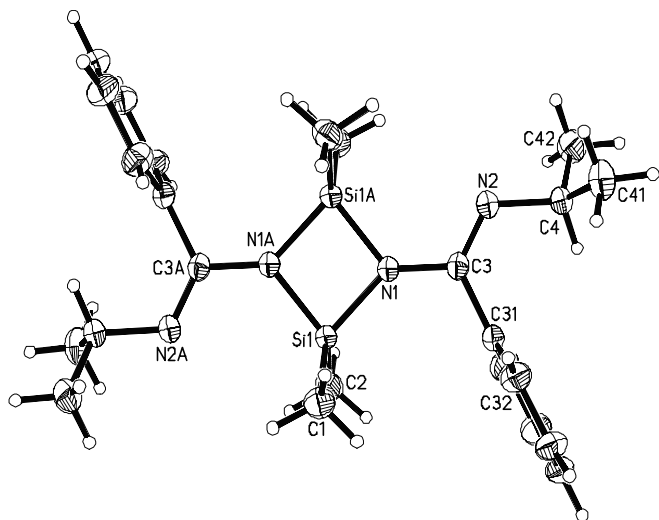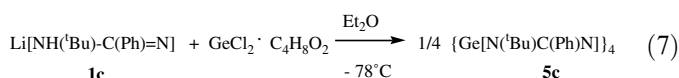
Fig. 3. Molecular structure of compound **5c** (a: view from above, b: side view; ORTEP drawing with 50% probability ellipsoids; substituent carbon atoms are depicted as wire-frame model for clarity). Selected bond distances (Å) and angles (°): Ge1–N1 2.043(1), Ge1–N2 1.990(1), Ge2–N21 1.994(1), Ge2–N22 2.040(1), Ge2–N2 1.901(1), Ge1A–N21 1.902(1); N1–C1–N2 110.4(1), N2–Ge1–N1 65.42(5), C1–N1–C2 131.6(1), C1–N1–Ge1 90.92(9), C2–N1–Ge1 136.61(10), N21A–Ge1–N1 92.87(5), C1–N2–Ge1 93.03(9), C1–N2–Ge1 92.74(9), Ge1–N2–Ge2 134.16(7), C20–N21–Ge1A 132.48(19), C20–N21–Ge2 92.88(9), Ge1A–N21–Ge2 134.67(7), C20–N22–C21 131.9(1), C20–N22–Ge2 90.97(9), C21–N22–Ge 136.0(1), N2–Ge2–N21 91.02(5), N21–Ge2–N22 64.41(5), N21A–Ge1–N2 91.03(5).

Therefore, a X-ray diffraction study of **5c** was undertaken, which revealed indeed the presence of the latter type of arrangement in the molecule, leading to four germanium spirocycles at four edges of an eight-membered ring, consisting of four-membered, almost planar, chelating amidinate rings at Ge, whose "free" (non-^{t}Bu substituted) N atoms bridge the Ge atoms and thus generating the eight-membered, centrosymmetric ring, in common for the four Ge-spirocenters. The molecular structure is shown in Fig. 3, together with selected bond distances and angles. The quite unusual conformation of the puckered eight-membered ring at first glance seemed to be due to steric needs: all phenyl groups are in an axial, all ^{t}butyl groups in an equatorial position. At closer sight, however, comparison can be made with the related structure of (NSF)$_4$ [24,25]: [NX$_3$(sp^2)]$_2$Ge(IV) *vs.* [F,NX$_2^-$(sp^2)]S(IV) and similar comparison holds, including also the 16-membered macrocycle, for the aforementioned tin compound [23]. Thus electronic needs seem to favor this elusive conformation.

Formal cyclotetramerisation of cyclic germanium(II) amidindiide {Ge[N(^{t}Bu)–C(Ph)–N]} *via* the Ge–N linkage defines intramolecular [Ge1–N1(^{t}Bu) 2.043(1)/Ge2–N22(^{t}Bu) 2.040(1) and Ge1–N2 1.990(1)/Ge2–N21 1.994(1)] and intermolecular [Ge2–N2 1.901(1)/Ge1–

N21# 1.902(1) Å] Ge–N distances, the latter being the shortest due to the formal negative charge on nitrogen and some ring strain in the four-membered chelate rings incorporating the essentially planar N1, C1, N2/N21, C20, N22 and the pyramidal Ge1/Ge2 atoms. Within these rings, the C–N distances represent delocalized, somewhat elongated double bonds (C1–N1 1.323(2)/C20–N21 1.329(2) and C1–N2 1.331(2)/C20–N22 1.324(2) Å), in remarkable contrast to **s3a** and **a4b**, and the N–C–N angles (N1–C1–N2 110.4(1)/N21–C20–N22 110.6(1)°) correspond to the more acute N–Ge–N angles (N1–Ge1–N2 65.4(1)/N21–Ge2–N22 65.4(1)°), whereas the *endo*-chelate angles at N(C1–N1–Ge1 90.9(1)/C1–N2–Ge1 93.0(1) and C20–N22–Ge2 91.0(1)/C20–N21–Ge2 92.9(1)°) deviate only slightly from 90°, in line with the other angles around Ge. As the other angles of the chelating C1/C20 and N1, N2/N21, N22 ring atoms add to planarity, the sp^2 carbon atoms seem more "resistant" (harder) to the needs of chelate ring formation than the sp^2 nitrogen atoms. And in line with expectation from **s3a** and **a4b**, the phenyl rings adopt an almost perpendicular position to the planes at C1/C20 (interplane angles N1–C1–N2/phenyl ring 63.3° and N21–C20–N22/phenyl ring 34.7°).
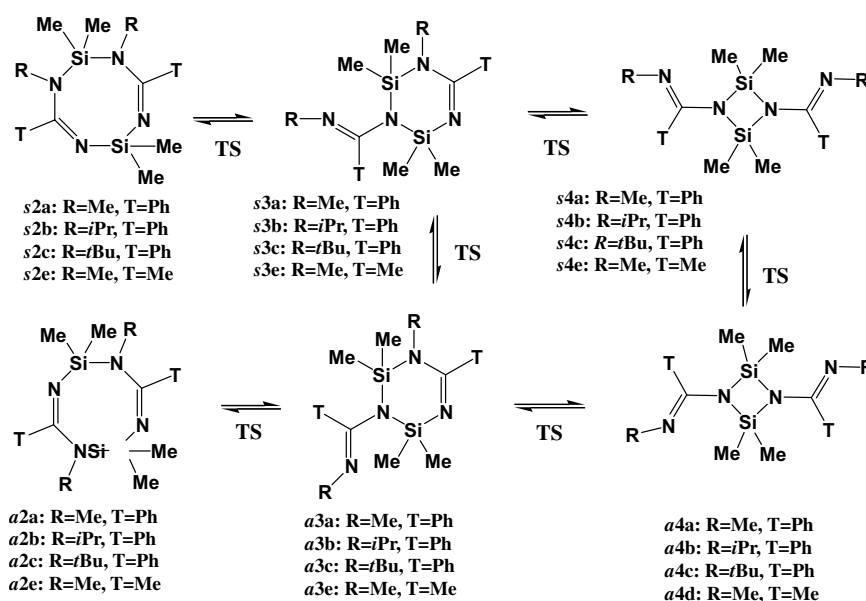
Scheme 1. Overview of the calculated pathways.

Table 1
Free energies (ΔG, kcal/mol) of all ring isomers (relative to the six-membered anti compounds **a3a**, **a3b**, **a3c**, or **a3e**, respectively)

Ring size →	8 (anti)	6 (anti)	4 (anti)	8 (syn)	6 (syn)	4 (syn)
R = Me, T = Ph	+6.5 (**a2a**)	0.0 (**a3a**)	−0.9 (**a4a**)	+8.1 (**s2a**)	−0.4 (**s3a**)	−2.0 (**s4a**)
R = ^{i}Pr, T = Ph	+11.7 (**a2b**)	0.0 (**a3b**)	−11.8 (**a4b**)	+14.4 (**s2b**)	−0.1 (**s3b**)	−10.7 (**s4b**)
R = ^{t}Bu, T = Ph	+17.1 (**a2c**)	0.0 (**a3c**)	−12.6 (**a4c**)	+19.4 (**s2c**)	+0.3 (**s3c**)	−11.6 (**s4c**)
R = Me, T = Me	+6.4 (**a2e**)	0.0 (**a3e**)	−1.5 (**a4e**)	+10.1 (**s2e**)	−2.3 (**s3e**)	−1.9 (**s4e**)
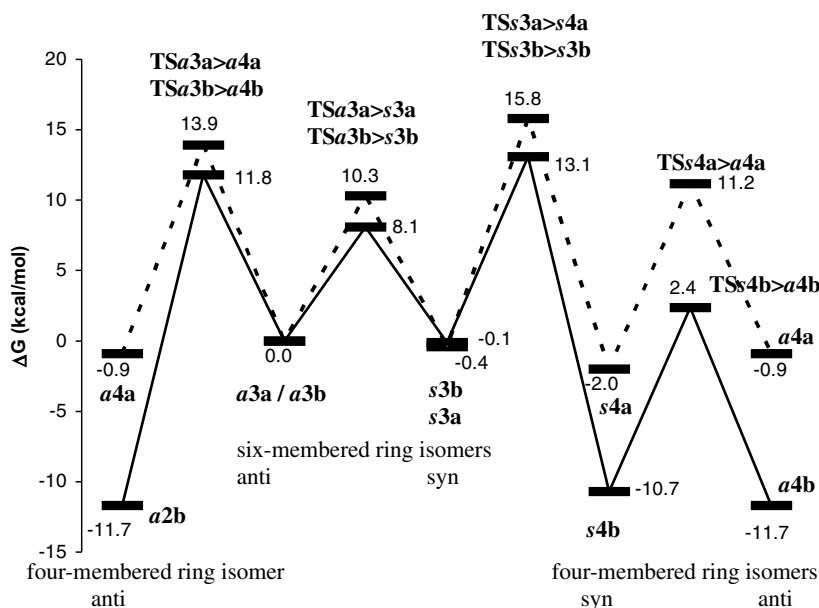
Scheme 2. Reaction pathways for R = ^{i}Pr (solid line) and R = Me (dashed line). The pathways to (or from) the eight-membered rings have been omitted for clarity.

3. DFT calculations

To determine the preferred ring size of the silicon–nitrogen heterocyclic compounds **2**–**4** in dependence of the *N*- and *C*-substituents, DFT calculations (B3LYP/6-31G*) were carried out to compare the energies of the four-, six-, and eight-membered isomers and to locate the transition states for the transformation between different ring sizes (see Scheme 1).

But not only the ring size itself leads to different isomers, furthermore *syn*-/*anti*-conformers for the four- and the six-membered rings have to be considered (see Scheme 1). The relative free energies of the ground states of the two experimentally investigated systems (**a**: R = Me/T = Ph, **b**: R = ^{i}Pr/T = Ph) and of the two systems studied only computationally (**c**: R = ^{t}Bu/T = Ph, **e**: R = T = Me) are given in Table 1.

From Table 1 it is evident, that the originally postulated eight-membered ring [1] is endergonic compared to the smaller ring isomers. The larger isopropyl substituent favors the four-membered ring by 11–12 kcal/mol with respect to the six-membered ring. Additionally, the four-membered *anti* (*a***4b**) ring conformer is 1.1 kcal/mol more exergonic than the *syn* (*s***4b**) compound. This is in agreement with the crystal structure that could be determined for compound *a***4b**.

For R = Me the energy differences between the four- and the six-membered rings are smaller with only 1–2 kcal/mol. In this case the *syn* conformer of the four-membered ring (*s***4a**) is the most exergonic species. Experimentally a crystal structure of the six-membered ring (*syn*) *s***3a** was determined. This might be a result

of the barrier height for the formation of the different species, we therefore took a look at the kinetics and the location of the transition states in order to explain the experimental result.

Scheme 2 gives an overview over the reaction pathways for the conversion between the four- and the six-membered compounds for the two experimentally investigated systems. Eq. (8) gives an example for the conversion of the (*syn*) six-membered ring to the corresponding four-membered isomer. Also the two rotational transition states that connect the *syn* and the *anti* conformers of the two ring systems have been considered (see Eq. (9)).

Atomic distances:
Si1-N1 1.95
Si1-N2 2.11
Si2-N2 1.73
N1-C1   1.34
N2-C1   1.32

Atomic distances:
Si1-N1 1.93
Si1-N2 2.15
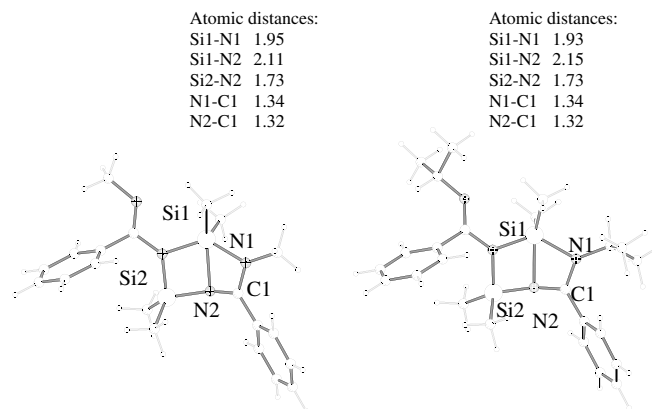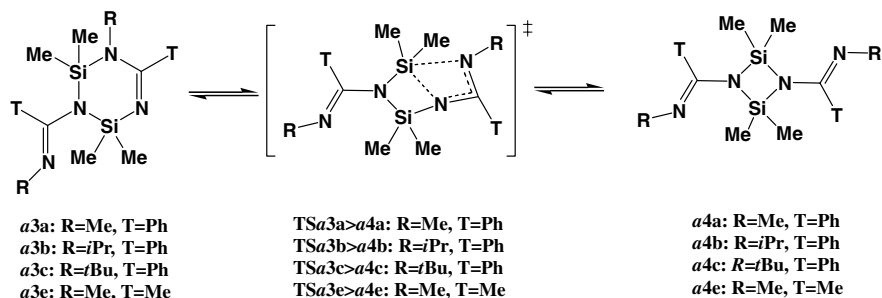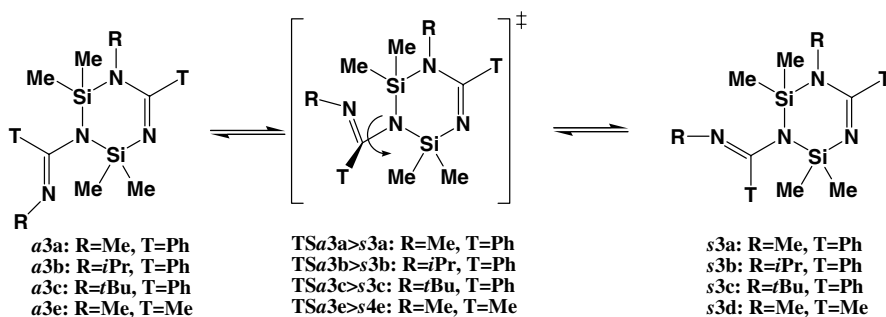Si2-N2 1.73
N1-C1   1.34
N2-C1   1.32

Fig. 4. Transition states **TS***s***3a** > *s***4a** (left) and **TS***s***3b** > *s***4b** (right) together with selected atomic distances.

a3a: R=Me, T=Ph
a3b: R=iPr, T=Ph
a3c: R=tBu, T=Ph
a3e: R=Me, T=Me

TSa3a>a4a: R=Me, T=Ph
TSa3b>a4b: R=iPr, T=Ph
TSa3c>a4c: R=tBu, T=Ph
TSa3e>a4e: R=Me, T=Me

a4a: R=Me, T=Ph
a4b: R=iPr, T=Ph
a4c: R=tBu, T=Ph
a4e: R=Me, T=Me

(8)

a3a: R=Me, T=Ph
a3b: R=iPr, T=Ph
a3c: R=tBu, T=Ph
a3e: R=Me, T=Me

TSa3a>s3a: R=Me, T=Ph
TSa3b>s3b: R=iPr, T=Ph
TSa3c>s3c: R=tBu, T=Ph
TSa3e>s4e: R=Me, T=Me

s3a: R=Me, T=Ph
s3b: R=iPr, T=Ph
s3c: R=tBu, T=Ph
s3d: R=Me, T=Me

(9)

The barrier heights for the conversion of the six-membered rings to the four-membered isomers are similar for R = Me (**TSa3a > a4a**, 13.9 kcal/mol and **TSs3a > s4a**, 15.8 kcal/mol) and R = ^{i}Pr (**TSa3b > a4b**, 11.8 kcal/mol and **TSs3b > s4b**, 13.1 kcal/mol). While in the case of the isopropyl substituent the lower barrier leads to the thermodynamically most favorable species, which has also been observed in the crystal structure, the situation is different for the methyl substituent. The ground states are energetically less favored by about 10 kcal/mol and the thermodynamically most favorable species **s4b** has to overcome higher barriers than what is needed for the formation of **s3a**, which was observed in the crystal structure. But the small energy differences of the isomers also call for a rapid conversion in solution as there is no species which is really favored thermodynamically. The structures of the transition states **TSs3a > s4a** and **TSs3b > s4b** are compared in Fig. 4. They are very similar, only small differences in the Si1–N2 and Si1–N1 distances can be observed.
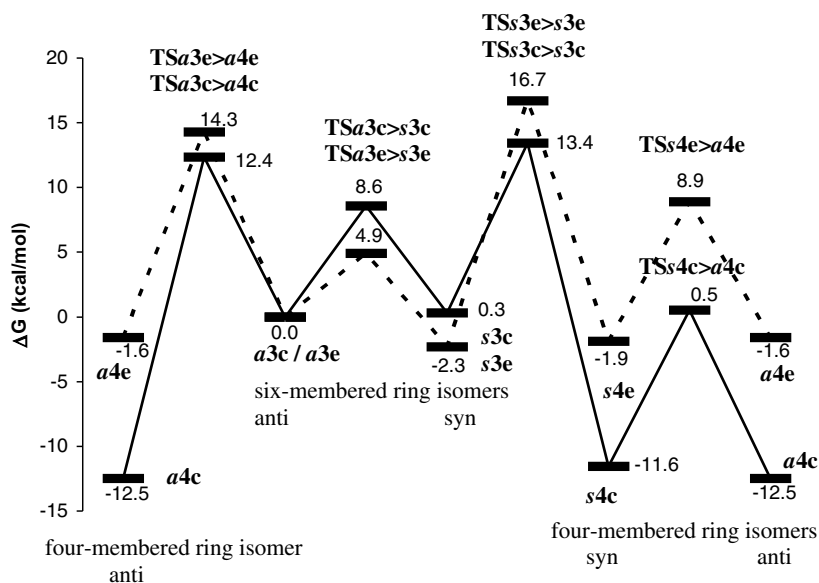
Scheme 3. Reaction pathways for the system R = ^{t}Bu/T = Ph (solid line) and R = T = Me (dashed line). The pathways to (or from) the eight-membered rings have been omitted for clarity.

For the sterically more demanding R = ^{t}Bu an even more exergonic formation of the four-membered ring is predicted. In analogy to what was observed for the isopropyl group, the anti isomer $a4c$ is the most feasible species (Scheme 3). To check whether the substituent T on the carbon atom can exert an influence we changed the phenyl substituent in system a (T = Ph, R = Me) to the smaller methyl group (e: R = T = Me). For the methyl/methyl compounds (e) the different isomers show no real preferred conformation, a mixture of more than one of the isomers and rapid interconversion is predicted for that substituent combination.

4. Conclusion

The deprotonation of N–H amidinates at silicon centers by a base is very sensitive to steric influences. With N-methyl or N-^{i}propyl substituents, six- or four-membered ring dimers may be obtained, with N-^{t}butyl substituents, deprotonation needs the bigger coordination center Ge(II), whereby a tetrameric arrangement is formed. Formation of eight-membered ring dimers, as described in the earlier literature, is not reproducible. Nevertheless, in line with earlier observations on the fluctional nature of amidinate ligands at silicon centers, low energy pathways exist for the mutual rearrangement of those dimeric ring molecules via higher coordination numbers at silicon and the four-, six- and eight-membered rings differ energetically, together with their respective rotational isomers, not grossly. The existing differences favor the four-membered rings, unless the C- and N-substituents are very small (C–Me, N–Me: six-membered ring). Obviously, solid-state effects may overcome this small difference and lead also to a six-membered ring for C–Ph, N–Me substitution.

In order to achieve the amidinate bridge formation in polymeric silicon compounds, the size of the C and N substituents must be reduced further. Hydrogen substituted or cyclic amidinates would be candidates for further studies in this field.

5. Experimental

5.1. General

All operations were performed under an atmosphere of dry, oxygen free nitrogen and with thoroughly dried glassware by means of standard high-vacuum-line techniques. Solvents were distilled under nitrogen from K–Na alloy. Elemental analyses were performed with a Vario EL CHN analyzer of the *Analytisches Laboratorium der TU München*. In our hands, silicon compounds of this kind tend to form silicon carbide during combustion and consequently, elemental analysis data are not reliable, particularly so for carbon. Therefore, additional mass spectra were recorded for analytical purposes. Chemical ionisation (CI) mass spectral data were obtained employing a Varian Mat 311A spectrometer; peaks are reported as m/z (assign-

ment, relative intensity). NMR spectra were recorded on a JEOL GX 270 spectrometer (^{1}H 270.17, ^{13}C{^{1}H} 67.94 MHz). Chemical shifts refer to TMS ($\delta = 0$) as internal standard and are reported in ppm, coupling constants J in Hz. Measurements were carried out in C_6D_6 (25 °C) and/or at varied temperatures in [d_8] toluene.

Amidinates $1a$, $1b$, $1d$ [6] were prepared as described in the literature, $1c$ according to this procedure [3]. All reagents, including Me_2SiCl_2 and $GeCl_2 \cdot$ dioxane, were from commercial sources and purified, when necessary.

5.2. {$Me_2Si[N–C(Ph)–N(Me)]\}_2$ ($s3a$)

To a solution of 21.25 mmol $MeNH_2$ (0.66 g) in 50 ml Et_2O were added 6.06 ml of a 1.65 molar solution of ^{n}BuLi in hexane (10 mmol) at −78 °C by means of a pipette. Slowly, the reaction mixture is allowed to warm to r.t. and after 20 h, the solvent and excess $MeNH_2$ was removed *in vacuo*. The residue was again suspended in 50 ml of Et_2O and at −78 °C, 9.80 mmol of PhCN (1.01 g) were added under stirring. After warming to r.t. and further stirring for 1 h, 9.80 mmol of NEt_3 (0.99 g) were added. After 1 h and cooling to −78 °C, 9.80 mmol of Me_2SiCl_2 (1.26 g) were added and again allowed to warm to r.t. After 18 h, volatiles were removed *in vacuo* and the solid, white residue was extracted with several portions of pentane (50 ml). Slow evaporation of the solvent followed by cooling to 10 °C for several days afforded large, colorless crystals (m.p. 138 °C) of $s3a$ Yield: 1.62 g (86.9%). $C_{20}H_{28}N_4Si_2$: MS(CI, 150 eV): m/z (%): 381 (90) [M], 365 (100) [M−Me], 349 (17) [M−2Me], 191 (29) [$Me_2SiNC(Ph)=NMe$], 174 (6) [$MeSiNC(Ph)=NMe$]. ^{1}H NMR ([d_8]toluene): Si(CH_3): −80 °C: δ 0.24 [s, 6H], 0.81 [s, 6H]; −60 °C: δ 0.28 [s, 6H], 0.74 [s, 6H]; 40 °C: δ 0.12 [s, 6H], 0.57 [s, 6H]; 60 °C: δ 0.15 [s (br), 6H], 0.57 [s (br), 6H]; 85 °C: δ 0.17 [s, 6H], 0.42 [s, 6H]; –N(CH_3): −80 °C: δ 2.37 [s, 1H, –N(H–CH$_2$)], 2.40 [s, 2H, –N(HC–H_2)], 2.97 [s, 3H, =NCH_3]; −60 °C: δ 2.45 [s, 3H, –N(CH_3)], 2.93 [s, 3H, =N(CH_3)]; 40 °C: δ 2.65 [s (br), 6H]; 60 °C: δ 2.65 [s, 6H]; 85 °C: δ 2.60 [s, 6H]; –C$_6H_5$: −80 to 85 °C: δ 6.93–7.18 [m, 10H]. ^{13}C{^{1}H} NMR (C_6D_6, 25 °C): δ 0.97 [s, Si(CH_3)], 25.24 [s, N(CH_3)], 127.28 [s, p-C_6H_5], 128.81 [s, m-C_6H_5], 129.00 [s, o-C_6H_5], 137.21 [s, i-C_6H_5]; ^{29}Si{^{1}H} NMR (C_6D_6, 25 °C): δ −0.52 (s). Anal. Calc. for $C_{20}H_{28}N_4Si_2$: C, 63.11; H, 7.41; N, 14.72. Found: C, 60.02; H, 7.80; N, 12.93%.

5.3. [$Me_2SiNC(Ph) = N^iPr]_2$ ($a4b$)

The analogous procedure as for $s3a$ was used, but Me_2SiCl_2 was added at r.t. and for the extraction, toluene was used. Reagents: 15.23 mmol ^{i}PrNH$_2$ (0.9 g), 13.09 mmol (7.7 ml of 1.7 molar solution) of ^{n}BuLi, 13.07 mmol PhCN (1.53 g), 13.04 mmol NEt$_3$ (1.32 g), 9.8 mmol Me_2SiCl_2 (1.26 g). Colorless crystals (m.p. 146 °C) are obtained. Yield:1.04 g, 36.5%. $C_{24}H_{36}N_4Si_2$: MS (CI, 150 eV): m/z (%): 436 (63) [M], 393 (33) [M−^{i}Pr],

318 (100) [M−2Me, −2^{i}Pr], 290 (15) [M−4Me, −2^{i}Pr], 219 (36) [Me$_2$SiNC(Ph)=N^{i}Pr]. ^{1}H NMR (C$_6$D$_6$, 25 °C): δ 0.48 (s, 12H, SiCH_3), 1.12 (d, 12H, $^3J = 6.7$, CH_3CH), 3.27 (sept, 2H, $^3J = 6.7$, CH$_3$CH), 7.04 [m, C$_6H_5$]. ^{13}C{^{1}H} NMR (C$_6$D$_6$, 25 °C): δ 1.79 (SiCH$_3$), 25.45 (CH$_3$CH), 50.31 (CH$_3$$C$H), 127.12 (p-$C_6H_5$), 128.18 (m-$C_6H_5$), 128.47 (o-$C_6H_5$), 138.01 (i-$C_6H_5$), 158.01 (N$C$N). ^{29}Si{^{1}H} NMR (C$_6$D$_6$, 25 °C): δ 3.88. Anal. Calc. for C$_{24}$H$_{36}$N$_4$Si$_2$: C, 66.00; H, 8.31; N, 12.83. Found: C, 61.61; H, 8.09; N, 11.60%.

5.4. {Ge[N(^{t}Bu)C(Ph)N]}$_4$ (5c)

To a suspension of 5.76 mmol Li[NH(^{t}Bu)−C(Ph)=N] (1.05 g) in 50 ml Et$_2$O was added slowly 2.88 mmol GeCl$_2 \cdot$ dioxane (0.67 g) at −78 °C under stirring and the mixture allowed to warm to r.t. After 20 h, the solvent was removed in vacuo and the residue extracted several times with pentane. The combined pentane (50 ml) solutions contained a brown, solid residue (0.31 g): NH(^{t}Bu)−C(Ph)=NH and 5c after drying (NMR). The solid residue of the former extraction was extracted with several portions of toluene. The combined toluene solu-

tions (70 ml) gave colorless crystals of 5c (m.p. 186 °C) after slowly evaporating the solvent to dryness. Yield 0.31 g (60%). In an independent experiment, DBU in THF was used as a base and 5c was obtained in 89.7% yield. C$_{44}$H$_{56}$N$_8$Ge$_4$: MS (^{74}Ge, CI, 150 eV): m/z (%): 989 (25) [M], 249 (10) [M/4], 177 (100) [H$_2$NC(Ph)NH^{t}Bu]. ^{1}H NMR (C$_6$D$_6$, 25 °C): δ 1.15 (s, 36H, CCH_3), 7.16–7.62 (m, 20H, C$_6H_5$). ^{13}C{^{1}H} NMR (C$_6$D$_6$, 25 °C): δ 32.14 (CCH$_3$), 52.47 (CCH$_3$), 125.94, 127.63, 129.31, 177.97 (C$_6$H$_5$), 164.23 (NCN). Anal. Calc. for C, 53.52; H, 5.72; N, 11.35. Found: C, 52.68; H, 5.82; N, 10.70%.

5.5. X-ray crystallography

Crystals of s3a, a4b, and 5c were prepared under argon in a matrix of perfluorinated polyether. Specimens of suitable quality and size were mounted on the ends of quartz fibers in F06206R oil and used for measurements of precise cell constants and intensity data collection on a Nonius DIP2020 diffractometer, using graphite-monochromated Mo Kα radiation ($\lambda = 0.71073$ Å). The structures were solved by a combination of direct methods (SHELXS-97 [26]) and difference-Fourier syntheses and refined by full matrix

Table 2
Crystal data, data collection, and structure refinement for compounds s3a, a4b, and 5c

	s3a	a4b	5c
Crystal data			
Formula	C$_{20}$H$_{28}$N$_4$Si$_2$	C$_{24}$H$_{36}$N$_4$Si$_2$	C$_{44}$H$_{56}$Ge$_4$N$_8$
M$_r$	320.64	436.75	987.33
Crystal system	Orthorhombic	Monoclinic	Monoclinic
Space group	Pna2$_1$	P2$_1$/c	C2/c
a (Å)	14.3687(3)	8.6880(2)	23.1928(3)
b (Å)	9.9001(2)	8.9290(2)	10.2179(1)
c (Å)	15.1940(3)	16.6550(5)	23.2167(2)
α (°)	90	90	90
β (°)	90	97.642(1)	90.232(1)
γ (°)	90	90	90
V (Å^3)	2161.4(1)	1280.5(1)	5501.9(1)
ρ_{calc} (g cm^{-3})	1.170	1.133	1.192
Z	4	2	4
F(000)	816	472	2016
μ(Mo Kα) (mm^{-1})	0.175	0.156	2.197
Data collection			
T (K)	143	143	143
h k l Range	0 → 18, 0 → 12, −19 → 0	0 → 10, 0 → 11, −21 → 20	0 → 30, 0 → 13, −30 → 29
Measured reflections	71646	2703	82580
Unique reflections [R$_{int}$]	2470 [0.030]	2703 [0.039]	6300 [0.037]
Reflections used for refinement	2470	2703	6300
Refinement			
Refined parameters	235	140	366
Final R values [$I \geqslant 2\sigma(I)$]			
R$_1$[a]	0.0341	0.0389	0.0240
wR$_2$[b]	0.0950	0.0998	0.0588
Absolute structure parameter	0.096	–	–
(shift/error)$_{max}$	<0.001	<0.001	<0.001
(e Å^{-3})	0.208/−0.274	0.203/−0.330	0.269/−0.410

$w = 1/[\sigma^2(F_o^2) + (ap)^2 + bp]$; $p = (F_o^2 + 2F_c^2)/3$; $a = 0.0743$ (s3a), 0.0492 (a4b), 0.0368 (5c); $b = 0.21$ (s3a), 0.57 (a4b), 0.62 (5c).
[a] $R = \sum(|F_o| - |F_c|)/\sum|F_o|$.
[b] $wR_2 = \{[\sum w(F_o^2 - F_c^2)^2]/\sum[w(F_o^2)^2]\}^{1/2}$.

least-squares calculations on F^2 (SHELXL-97 [26]). In the case of **5c** the scattering contribution of unidentified and highly disordered solvent in voids of the crystal structure was accounted for by means of the program SQUEEZE [27]. It was carefully checked, that this treatment did not affect the structural parameters: details are given in the supporting information. The thermal motion was treated anisotropically for all non-hydrogen atoms. All hydrogen atoms were calculated and allowed to ride on their parent atoms with fixed isotropic contributions. Further information on crystal data, data collection and structure refinement are summarized in Table 2. Important interatomic distances and angles are shown in the corresponding figure captions.

5.6. DFT calculations

All calculations were performed with the software package GAUSSIAN03 [28] using the density functional/Hartree–Fock hybrid model Becke3LYP [29–32] and the split valence double-ζ (DZ) basis set 6-31G* [33–35]. No symmetry or internal coordinate constraints were applied during optimizations. All reported intermediates were verified as true minima by the absence of negative eigenvalues in the vibrational frequency analysis. Transition-state structures were located using the Berny algorithm [36] until the Hessian matrix had only one imaginary eigenvalue. The identity of all transition states was confirmed by IRC calculations and by animating the negative eigenvector coordinate with MOLDEN [37] and GaussView [38].

Approximate free energies (ΔG) and enthalpies (ΔH) were obtained through thermochemical analysis of frequency calculations, using the thermal correction to Gibbs free energy as reported by GAUSSIAN-03. This takes into account zero-point effects, thermal enthalpy corrections and entropy. All energies reported in this paper, unless otherwise noted, are free energies or enthalpies at 298 K, using unscaled frequencies. All transition states are maxima on the electronic potential energy surface (PES), which may not correspond to maxima on the free energy surface.

Acknowledgments

Appendix A. Supplementary material

CCDC 636083, 626000 and 636082 contain the supplementary crystallographic data for **s3a**, **a4b** and **5c**. These data can be obtained free of charge via http://www.ccdc.cam.ac.uk/conts/retrieving.html, or from the Cambridge Crystallographic Data Centre, 12 Union Road, Cambridge CB2 1EZ, UK; fax: (+44) 1223-336-033; or e-mail: deposit@ccdc.cam.ac.uk. Supplementary data associated with this article can be found, in the online version, at doi:10.1016/j.jorganchem.2007.02.032.

References

[1] O.J. Scherer, P. Hornig, Angew. Chem. 79 (1967) 60.
[2] H.H. Karsch, P.A. Schlueter, in: N. Auner, J. Weis (Eds.), Organosilicon Chemistry IV – From Molecules to Materials, Wiley-VCH, Weinheim, 2000, p. 287.
[3] T. Segmüller, PhD thesis, Technische Universität, München, 2003.
[4] H.H. Karsch, T. Segmüller, in: N. Auner, J. Weis (Eds.), Organosilicon Compounds VI – From Molecules to Materials, Wiley-VCH, Weinheim, 2005, p. 194.
[5] H.H. Karsch, T. Segmueller, in: N. Auner, J. Weis (Eds.), Organosilicon Chemistry V – From Molecules to Materials, Wiley-VCH, Weinheim, 2003, p. 270.
[6] O.J. Scherer, P. Hornig, Chem. Ber. 101 (1968) 2533.
[7] H.H. Karsch, P.A. Schlueter, in: N. Auner, J. Weis (Eds.), Organosilicon Chemistry III – From Molecules to Materials, Wiley-VCH, Weinheim, 1998, p. 53.
[8] H.H. Karsch, F. Bienlein, in: N. Auner, J. Weis (Eds.), Organosilicon Chemistry II – From Molecules to Materials, Wiley-VCH, Weinheim, 1995, p. 133.
[9] P.J. Wheatley, J. Chem. Soc. (1962) 1721.
[10] L. Parkanyi, G. Argay, P. Hencsei, J. Nagy, J. Organomet. Chem. 116 (1976) 299.
[11] W. Clegg, U. Klingebiel, G.M. Sheldrick, N. Vater, Z. Anorg. Allg. Chem. 482 (1981) 88.
[12] L. Bihatsi, P. Hencsei, L. Parkanyi, J. Organomet. Chem. 219 (1981) 145.
[13] W. Clegg, U. Klingebiel, G.M. Sheldrick, Z. Naturforsch. 37B (1982) 423.
[14] A. Szollosy, L. Parkanyi, L. Bihatsi, P. Hencsei, J. Organomet. Chem. 251 (1983) 159.
[15] W. Clegg, M. Haase, G.M. Sheldrick, N. Vater, Acta Crystallogr., Sect. C 40 (1984) 871.
[16] N. Auner, E. Herdtweck, E. Penzenstaudler, Acta Crystallogr., Sect. C 49 (1993) 359.
[17] L. Parkanyi, L. Bihatsi, P. Hencsei, Z. Kristallogr. 209 (1994) 905.
[18] S.A.A. Shah, H.W. Roesky, P. Lubini, H.-G. Schmidt, Acta Crystallogr., Sect. C 52 (1996) 2810.
[19] H.H. Karsch, P.A. Schlueter, M. Reisky, Eur. J. Inorg. Chem. (1998) 433.
[20] S.R. Foley, C. Bensimon, D.S. Richeson, J. Am. Chem. Soc. 119 (1997) 10359.
[21] S.R. Foley, Y. Zhou, G.P.A. Yap, D.S. Richeson, Inorg. Chem. 39 (2000) 924.
[22] M. Veith, Angew. Chem. 99 (1987) 1.
[23] M. Veith, M. Grosser, J. Organometal. Chem. 229 (1982) 247.
[24] G.A. Wiegers, A. Vos, Acta Crystallogr. 14 (1961) 562.
[25] G.A. Wiegers, A. Vos, Acta Crystallogr. 16 (1963) 152.
[26] G.M. Sheldrick, SHELXL-97 – Program for Crystal Structure Solution, Institut für Anorganische Chemie der Universität, Göttingen, Germany, 1997.
[27] A.L. Spek, Acta Crystallogr., Sect. A 46 (1990) C34.
[28] M.J. Frisch, G.W. Trucks, H.B. Schlegel, G.E. Scuseria, M.A. Robb, J.R. Cheeseman, J.A. Montgomery Jr., T. Vreven, K.N. Kudin, J.C. Burant, J.M. Millam, S.S. Iyengar, J. Tomasi, V. Barone, B. Mennucci, M. Cossi, G. Scalmani, N. Rega, G.A. Petersson, H. Nakatsuji, M. Hada, M. Ehara, K. Toyota, R. Fukuda, J. Hasegawa, M. Ishida, T. Nakajima, Y. Honda, O. Kitao, H. Nakai, M. Klene, X. Li, J.E. Knox, H.P. Hratchian, J.B. Cross, V. Bakken, C. Adamo, J. Jaramillo, R. Gomperts, R.E. Stratmann, O. Yazyev, A.J. Austin, R. Cammi, C. Pomelli, J.W. Ochterski, P.Y. Ayala, K. Morokuma, G.A. Voth, P. Salvador, J.J. Dannenberg, V.G. Zakrzewski, S. Dapprich, A.D. Daniels, M.C. Strain, O. Farkas, D.K. Malick, A.D. Rabuck, K. Raghavachari, J.B. Foresman, J.V. Ortiz, Q. Cui, A.G. Baboul, S. Clifford, J. Cioslowski, B.B. Stefanov, G. Liu, A. Liashenko, P. Piskorz, I. Komaromi, R.L. Martin, D.J. Fox, T. Keith, M.A. Al-Laham, C.Y. Peng, A. Nanayakkara, M. Challa-

combe, P.M.W. Gill, B. Johnson, W. Chen, M.W. Wong, C. Gonzalez, J.A. Pople, Gaussian 03, Revision C.02, Gaussian Inc., Wallington, CT, 2004.

[29] C. Lee, W. Yang, R.G. Parr, Phys. Rev. B: Condens. Matter 37 (1988) 785.

[30] S.H. Vosko, L. Wilk, M. Nusair, Can. J. Phys. 58 (1980) 1200.

[31] A.D. Becke, J. Chem. Phys. 98 (1993) 5648.

[32] P.J.D. Stephens, F.J. Devlin, C.F. Chabalowski, M.J. Frisch, J. Phys. Chem. 98 (1994) 11623.

[33] P.C. Hariharan, J.A. Pople, Theor. Chim. Acta 28 (1973) 213.

[34] M.M. Mancl, W.J. Petro, W.J. Hehre, J.S. Binkley, M.S. Gordon, D.J. DeFree, J.A. Pople, J. Chem. Phys. 77 (1982) 3654.

[35] V. Rassolov, J.A. Pople, M. Ratner, T.L. Windus, J. Chem. Phys. 109 (1998) 1223.

[36] H.B. Schlegel, J. Comp. Chem. 3 (1982) 214.

[37] G. Schaftenaar, J.H. Noordik, J. Comput.-Aided Mol. Des. 14 (2000) 123.

[38] R.I. Dennington, T. Keith, J.M. Millam, K. Eppinnett, W.L. Hovell, R. Gilliland, GaussView, Gaussian Inc., Wallingford, CT, 2003.